

Charge Transfer Reactions between Water Isotopologues and Kr⁺ ions

Andriana Tsikritea, Jake A. Diprose, Jérôme Loreau, and Brianna R. Heazlewood*

Cite This: *ACS Phys. Chem Au* 2022, 2, 199–205

Read Online

ACCESS |



Metrics & More



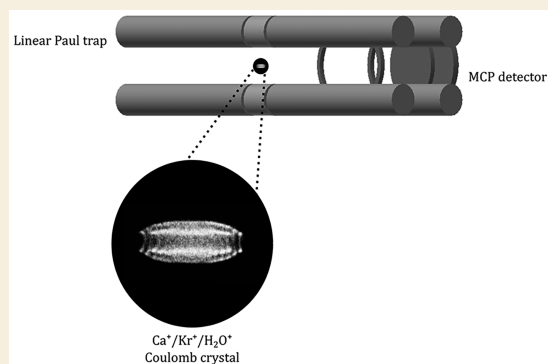
Article Recommendations



Supporting Information

ABSTRACT: Astrochemical models often adopt capture theories to predict the behavior of experimentally unmeasured ion–molecule reactions. Here, reaction rate coefficients are reported for the charge transfer reactions of H₂O and D₂O molecules with cold, trapped Kr⁺ ions. Classical capture theory predictions are found to be in excellent agreement with the experimental findings. A crossing point identified between the reactant and product potential energy surfaces, constructed from high-level *ab initio* calculations, further supports a capture-driven mechanism of charge transfer. However, ion–molecule reactions do not always agree with predictions from capture theory models. The appropriateness of using capture theory-based models in the absence of detailed experimental or theoretical studies is discussed, alongside an analysis of why capture theory is appropriate for describing the likelihood of charge transfer between Kr⁺ and the two water isotopologues.

KEYWORDS: *Coulomb crystals, reaction kinetics, ab initio calculations, capture theory models, astrochemistry*



INTRODUCTION

More than 200 molecular species have now been unambiguously identified in the interstellar medium (ISM),¹ and hundreds of deuterated analogues of these molecules have also been observed.² Ion–molecule reactions are expected to play an important role in the gas-phase chemistry occurring in the ISM, as these reactions often exhibit a negative trend with temperature, with enhanced rates at low temperatures.^{3,4} Spectroscopic observations have been critical in identifying species that are present in the ISM. However, in order to understand the chemistry of the ISM and to establish how the detected molecular species were formed, more details are required. To unravel the complex chemistry of the ISM, a collaborative effort is needed—combining laboratory studies and the development of detailed models with spectroscopic observations and astrochemical databases. There is a well-acknowledged lack of experimental data recorded under conditions relevant to the ISM, especially when considering deuterated analogues. As such, capture theories are often employed in astrochemical models to provide an estimate of the rate coefficients exhibited by experimentally unmeasured ion–molecule reactions.⁵

Capture theories have been found to successfully predict a number of experimentally measured rate coefficients over a temperature range that spans from >300 K down to 10 K.⁶ However, there are also examples of reaction systems for which capture theories cannot account for the likelihood of reaction. Such behavior was observed in the charge transfer of ammonia

isotopologues with rare-gas ions (Xe⁺, Kr⁺, and Ar⁺)—with the experimental rate coefficients consistently lower than those predicted by capture theory.^{7,8} The charge transfer processes also exhibited an unexpected inverse kinetic isotope effect (KIE): for all three rare-gas ions studied, ND₃ reacted faster than NH₃. Ammonia is known to be present in the ISM, with both ND₃ and NH₃ spectroscopically identified.⁹ Water is another small polar molecule found in the ISM, with both H₂O and D₂O identified.¹⁰ To establish whether kinetic isotope effects might be generally observed in charge transfer reactions involving rare-gas ions and small polar molecules, and to test the accuracy of capture theory in additional astrochemically relevant reaction systems, we considered the reactivity of water isotopologues.

In this work, we examine charge transfer reactions between thermal water (H₂O or D₂O) molecules and cold, trapped Kr⁺ ions. In both systems, the experimental reaction rate coefficients are found to be in good agreement with predictions from capture theory models. No kinetic isotope effects are observed; H₂O and D₂O exhibit very similar rate coefficients. Charge transfer therefore appears to be a capture-limited

Received: November 12, 2021

Revised: December 23, 2021

Accepted: December 29, 2021

Published: January 31, 2022



process, displaying a dependence on the strength of the long-range attractive forces between the neutral polar molecule and the ionic reactant. The success of capture theory models in describing the behavior of ion–molecule interactions is discussed—both in the context of the findings detailed in this work, and in more general terms.

METHODS

A. Experimental Section

Charge transfer reactions are studied within Ca^+ Coulomb crystals, following the same approach adopted in previous work.^{7,8} Briefly, Ca atoms, produced by a resistively heated oven, are nonresonantly ionized at the center of a linear Paul ion trap using the 355 nm output of a frequency-tripled Nd:YAG laser. The resulting Ca^+ ions are dynamically confined by a combination of radiofrequency and static voltages applied to the four cylindrical trap rods. A closed-cycle laser cooling scheme is implemented, with a 397 nm diode driving the $4s^2S_{1/2} \rightarrow 4p^2P_{1/2}$ transition and a 866 nm diode returning population (lost to the $^2D_{3/2}$ state) to the main cooling transition by exciting the $3d^2D_{3/2} \rightarrow 4p^2P_{1/2}$ transition. Once sufficient kinetic energy has been removed,¹¹ laser-cooled Ca^+ ions can form Coulomb crystals—adopting a regular 3-dimensional lattice-like structure. Fluorescence emitted as part of the laser cooling cycle is captured by a charge-coupled device (CCD) camera and 10 \times microscope objective lens. Figure 1 depicts Ca^+ Coulomb crystal images captured at different

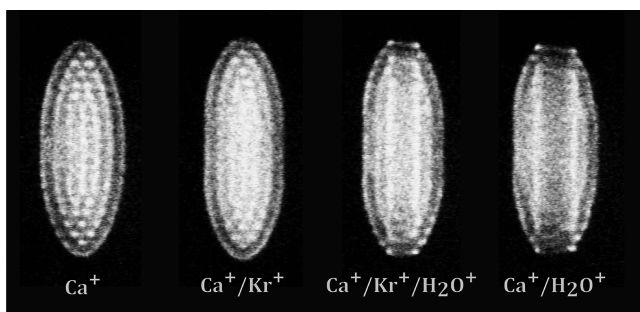


Figure 1. Coulomb crystal images at different times during a charge transfer reaction between Kr^+ ions and H_2O neutrals. Water molecules introduced to the ion trap volume initiate the reaction. The formation and growth of a dark core qualitatively shows the reaction progress.

times during a charge transfer reaction. Sympathetically cooled species (i.e., co-trapped ions that are translationally cold due to elastic collisions with the laser-cooled Ca^+ ions) do not fluoresce. However, the presence of co-trapped ions induces changes in the locations of the fluorescing Ca^+ ions within the Coulomb crystal, and these changes can be directly observed by the CCD camera in real time. Time-of-flight mass spectra (ToF-MS) are recorded by ejecting the ions toward a flight tube and onto a microchannel plate (MCP) detector.¹²

Kr atoms are introduced to the reaction chamber through a high-precision leak valve interfaced with a three-way pulsed valve system, admitting a constant and reproducible volume of gas.¹³ A (2 + 1) REMPI scheme at 212.6 nm, using the tripled output of a Nd:YAG-pumped dye laser, forms Kr^+ ions in the trap center. A time delay of ~ 15 s is introduced to allow for sympathetic cooling of the Kr^+ ions into the crystal, and to ensure that all Kr^+ ions are in the ground electronic state.^{8,11} Any Kr^+ ions produced in the higher energy $^2P_{1/2}$ spin state have a lifetime of only 340 ms, decaying to the ground $^2P_{3/2}$ state via a magnetic-dipole-allowed transition with an Einstein coefficient of $A_m = 2.8 \text{ s}^{-1}$.¹⁴

H_2O or D_2O vapor at 293 K is admitted to the reaction chamber through a second high-precision leak valve, initiating the charge transfer reactions. The product ions form a dark core, the growth of

which indicates the reaction progress (see Figure 1). Experimental images are compared with molecular dynamics simulations, yielding quantitative information on the crystals' composition as a function of the reaction time. To complement the imaging analysis, crystals are ejected from the ion trap at selected reaction times and ToF-MS traces are recorded—thereby confirming the mass-to-charge ratios and relative abundances of all ions in the crystal at the point of ejection. No competing reaction pathways are observed. Charge transfer is found to be a one-to-one process¹⁵ that follows a pseudo-first order kinetic model.^{7,8} Bimolecular rate coefficients are calculated assuming a constant water partial pressure, with the partial pressure established by calibrating the high-precision leak valve to an ion gauge and a residual gas analyzer (see Supporting Information for further details).

B. Potential Energy Surfaces

Potential energy surfaces (PESs) for the $\text{H}_2\text{O}-\text{Kr}^+$ system have been constructed by means of the multiconfigurational self-consistent field method and the multireference configuration interaction (MRCI) method including the Davidson correction, as implemented in the MOLPRO2018.1 quantum chemistry package.^{16–18}

H_2O in its ground electronic state (X^1A_1) has an HOH angle of $\theta_{\text{HOH}} = 104.5^\circ$ and a bond length $R_{\text{OH}} = 0.9576 \text{ \AA}$. For the cation H_2O^+ in its ground state (\tilde{X}^2B_1), $\theta_{\text{HOH}} = 110.46^\circ$ with bond length $R_{\text{OH}} = 0.9988 \text{ \AA}$. Due to the similarity in geometries, the O–H bond length and the HOH angle are kept fixed at the equilibrium value of H_2O in the present calculations. This leads to three-dimensional PESs, as discussed below.

The initial state, $\text{Kr}^+(^2P) + \text{H}_2\text{O}(^1A_1)$, gives rise to two $^2A'$ states and a $^2A''$ state in the C_s group, while the exit channel, $\text{Kr}(^1S) + \text{H}_2\text{O}^+(\tilde{X}^2B_1)$, leads to a $^2A''$ state in C_s , for a total of two $^2A'$ states and two $^2A''$ states (or four states in the C_1 group). We note that the first excited state, $\text{H}_2\text{O}^+(\tilde{A}^2A_1)$, has an ionization potential about 0.15 eV higher than Kr, and could therefore potentially be reached. However, the geometry of H_2O in this state is nearly linear (with bond length $R_{\text{OH}} = 0.98 \text{ \AA}$)—a very different geometry to what is seen in ground state H_2O^+ and ground state H_2O . As such, the excited \tilde{A}^2A_1 state is neglected in the present calculations.

The basis set used is aug-cc-pVTZ for all atoms. For the Kr atom the 10 innermost electrons are described by an effective core potential (ECP10MDF); the $3s^23p^63d^{10}$ orbitals are kept frozen. For the O atom the $1s^2$ orbitals are frozen. The active space consists of the remaining orbitals, that is, $4s^24p^6$ for Kr, $2s^22p^4$ for O, and $1s$ for each H atom. In the C_s point group, this leads to $7a'$ and $3a''$ core orbitals, with $7a'$ and $3a''$ additional orbitals in the active space. The spin-orbit splitting in Kr^+ (5370 cm^{-1}) is taken into account by diagonalizing the Breit–Pauli operator on the basis of MRCI wave functions.

RESULTS

Reaction Rate Coefficients

The experimental rate coefficients measured for the $\text{Kr}^+ + \text{H}_2\text{O}$ and $\text{Kr}^+ + \text{D}_2\text{O}$ reaction systems are $k_{\text{H}} = 1.8(7) \times 10^{-9} \text{ cm}^3 \text{ s}^{-1}$ and $k_{\text{D}} = 2(1) \times 10^{-9} \text{ cm}^3 \text{ s}^{-1}$, respectively. The reactions are assigned an effective temperature of 244 K for the $\text{Kr}^+ + \text{H}_2\text{O}$ system and 240 K for the $\text{Kr}^+ + \text{D}_2\text{O}$ system. This temperature represents a weighted average of the thermal water reactants (293 K in our laboratory) and the sympathetically cooled Kr^+ ions (at ≈ 15 K). The latter is estimated from molecular dynamics simulations and accounts for both the secular motion and the micromotion of the trapped ions.

The average dipole orientation (ADO) capture theory model is employed for comparison with the experimentally measured rate coefficients. ADO theory describes the interaction between ions and polar molecules in a capture framework, where any collision that leads to complex formation proceeds to products with unit probability. The

model assumes a classical distribution of rotational states for the neutral reactant.^{19,20} As our reactions take place at temperatures around 240 K, ADO is expected to approximately predict the rate of capture. Further details on the ADO calculations are provided in previous work;^{7,8} the constants and input parameters used in this work are set out in Table 2.

Experimental rate coefficients are set out in Table 1 and Figure 2, alongside the predicted values from the ADO

Table 1. Experimental and ADO Rate Coefficients for the Charge Transfer Reactions between Kr^+ and Two Water Isotopologues^a

reaction system	k_{exp} ($\text{cm}^3 \text{s}^{-1} \times 10^{-9}$)	$k_{\text{H}}/k_{\text{D}}$	k_{ADO} ($\text{cm}^3 \text{s}^{-1} \times 10^{-9}$)	T (K)
$\text{Kr}^+ + \text{H}_2\text{O}$	1.8(7)		1.98	244
$\text{Kr}^+ + \text{D}_2\text{O}$	2(1)	0.9(6)	1.90	240
$\text{Kr}^+ + \text{NH}_3$	0.51(5) ^b		1.82	246
$\text{Kr}^+ + \text{ND}_3$	1.0(3) ^b	0.5(2)	1.69	239

^aFindings reported in previous work, for the Kr^+ + ammonia reaction systems, are also given. Uncertainties are stated in parentheses (see Supporting Information for details on how the uncertainties are established), with the effective reaction temperatures specified. ^bTsikritea et al.⁸

Table 2. Polarizabilities,^{30–32} Dipole Moments,^{30,32,33} and c Parameters²⁰ Used to Calculate the ADO Rate Coefficients

isotopologue	α (cm^3)	μ_{D} (D)	c
H_2O	1.45×10^{-24}	1.848	0.254
D_2O	1.44×10^{-24}	1.851	0.254
NH_3	2.16×10^{-24}	1.47	0.227
ND_3	1.88×10^{-24}	1.50	0.232

calculations. Very similar rate coefficients are observed for the two isotopologues; Kr^+ ions react with H_2O and D_2O at a comparable rate. The experimental rate coefficients are in excellent agreement with the classical ADO theory calculations. As the reactions are studied under conditions for which classical descriptions hold, this agreement indicates that

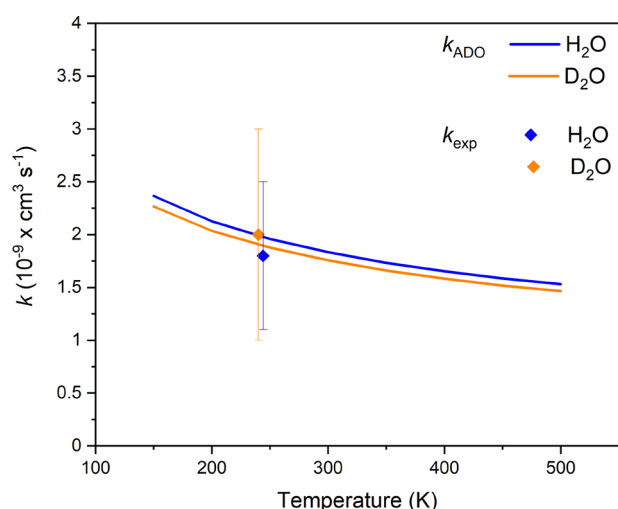


Figure 2. Charge transfer rate coefficients for the $\text{Kr}^+ + \text{H}_2\text{O}$ (blue) and $\text{Kr}^+ + \text{D}_2\text{O}$ (orange) reaction systems, as established from ADO capture theory models and from experimental measurements. Error bars indicate the uncertainty in the experimental rate coefficients (see Supporting Information for further details).

electron transfer is a capture-limited process. Other capture theory models are also consistent with the experimental rate coefficients. Details of these calculations are given in the Supporting Information. The relative magnitudes of the experimental rate coefficients given in Table 1 suggest that no KIE is present, with $k_{\text{H}}/k_{\text{D}} = 0.9(6)$.

These experimental results can be understood on the basis of three-dimensional PESs $V(R, \theta, \phi)$, where R is the length of the vector \mathbf{R} describing the position of the Kr atom (ion) with respect to the center of mass of H_2O^+ , θ is the angle between the vector \mathbf{R} and the C_2 axis of H_2O , and ϕ is the angle of rotation of this vector around the C_2 axis. The PESs have been constructed for several values of the angle ϕ by computing the energy for 26 values of the internuclear distance R between 3 a_0 and 15 a_0 , and 11 values of θ between 0° and 180° . The most favorable approach for $\text{H}_2\text{O} + \text{Kr}^+$ collisions is when $\theta = 0^\circ$, where the ion approaches along the negative end of the dipole vector. The potential energy curves for this orientation are shown in Figure 3. We observe the presence of a strong

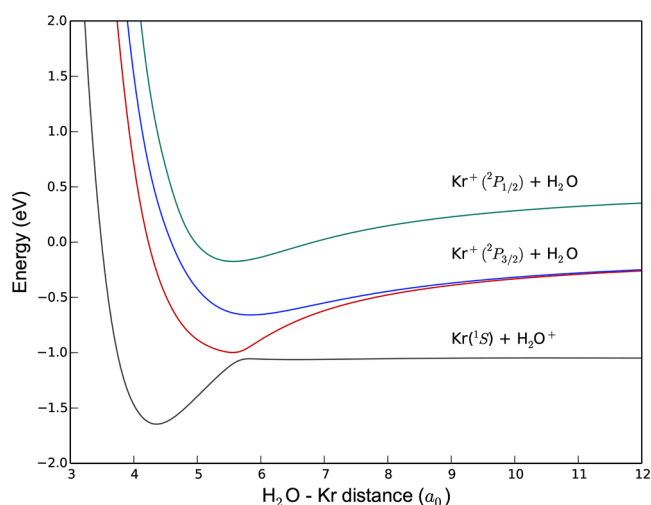


Figure 3. One-dimensional cut of the PESs of the $[\text{H}_2\text{OKr}]^+$ complex participating in the charge transfer process, as a function of the distance R between the Kr atom and the center of mass of H_2O . The angles are $\theta = \phi = 0^\circ$, corresponding to the Kr atom approaching along the negative side of the dipole of H_2O .

avoided crossing between the entrance and exit channels at a distance of $5.7a_0$, leading to an efficient charge transfer process. Collisions between the reactants at other orientations are less favorable. Two-dimensional PESs for the two lowest electronic states shown in Figure 3 are illustrated for $\phi = 0^\circ$ and $\phi = 90^\circ$ in Figure 4.

Other Reaction Pathways

Charge transfer is the only energetically accessible reaction pathway under the experimental conditions. The formation of ground-state H_2O^+ ions, $\text{Kr}^+(^2\text{P}_{3/2}) + \text{H}_2\text{O} \rightarrow \text{Kr} + \text{H}_2\text{O}^+(\tilde{X}^2\text{B}_1)$, has a reported exothermicity of $\Delta H = -1.38$ eV.¹⁵ All other reaction pathways, such as the hydrogen abstraction channel $\text{Kr}^+(^2\text{P}_{3/2}) + \text{H}_2\text{O} \rightarrow \text{KrH}^+ + \text{OH}$ ($\Delta H = 0.4$ eV), are endothermic.¹⁵ ToF-MS data confirm the absence of any competitive reaction channels, with only charge transfer product ions observed. While we are not aware of any previous studies on the $\text{Kr}^+ + \text{D}_2\text{O}$ reaction system, the absence of any KrD^+ ions in the ToF-MS traces suggests that this channel is also energetically closed for deuterated water. Most back-

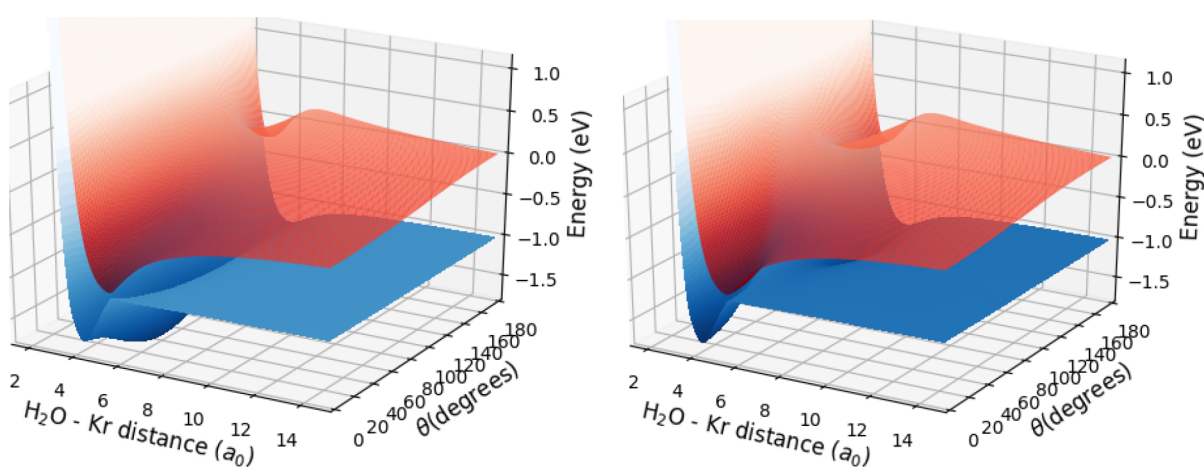


Figure 4. Two-dimensional PESs $V(R, \theta)$ of the lowest two electronic states of the $[\text{H}_2\text{OKr}]^+$ complex participating in the charge transfer process. Left panel, $\phi = 0^\circ$; right panel, $\phi = 90^\circ$.

ground gases in the reaction chamber are removed by a heat exchange device.^{7,8} Any remaining species are identified with a residual gas analyzer (RGA). Under the experimental conditions, reactions between Kr^+ ions and background species present in the reaction chamber are typically absent or negligible. If any such reactions do occur, they are monitored by ToF-MS, quantified using molecular dynamics simulations, and included in the kinetic model used to extract reaction rate coefficients. A detailed discussion on the treatment of background reactions can be found in previous work.^{7,8} Specific to this study, the possibility of hydrogen exchange with D_2O in the liquid reservoir (prior to admission of the reactant to the ion trap volume) is carefully monitored throughout the measurements using the RGA. The reservoir is refilled frequently, with the RGA confirming that there is minimal hydrogen exchange.

It should also be noted that Ca^+ ions within the Coulomb crystal—the laser-cooled species that sympathetically cool co-trapped ions—can themselves react with water to produce CaOH^+ (or CaOD^+) ions. The reaction involves Ca^+ ions in the metastable $3d^2D_{3/2}$ state, populated as part of the laser cooling cycle.²¹ To ensure that any side reactions are accurately taken into account, extensive background reaction studies between monocomponent Ca^+ Coulomb crystals and water neutrals (both H_2O and D_2O) have been conducted. Under the experimental conditions adopted in this work, the rate at which Ca^+ ions react with water is negligible on the time scale of the charge transfer reactions. On the few occasions when CaOH^+ or CaOD^+ ions are detected in the ToF traces, they are included in the analysis and explicitly taken into account.

DISCUSSION

Reaction Mechanism

The $\text{Kr}^+ + \text{H}_2\text{O}$ reaction has been previously studied at 296 K using the flowing afterglow technique, with a charge transfer rate coefficient of $k = 1.2(2) \times 10^{-9} \text{ cm}^3 \text{ s}^{-1}$ reported.²² It is unclear, however, if the Kr^+ ions in this earlier study were exclusively in the ground $^2P_{3/2}$ electronic state (as in this work), or whether a mixture of electronic states ($^2P_{3/2}$ and $^2P_{1/2}$) were populated. Additionally, the flowing afterglow experiments were carried out under different conditions to those adopted in this work—at pressures several orders of

magnitude higher, at a higher collision energy, and with a different distribution of internal energy in the reactants. As such, it is not possible to directly compare the rate coefficients reported from the earlier flowing afterglow study with the findings of this work.

Another study, undertaken at hyperthermal collision energies (spanning 0.1–10 eV) in an octopole guided ion-beam apparatus, did consider the reactivity of $\text{Kr}^+(^2P_{3/2})$ and $\text{Kr}^+(^2P_{1/2})$ separately.¹⁵ While the collision energies in the hyperthermal study are clearly very different to those employed in this work, the mechanistic insights that were reported are interesting. For the reaction of $\text{Kr}^+(^2P_{3/2})$ with H_2O , only ground state water ion products, $\text{H}_2\text{O}^+(\tilde{X}^2B_1)$, were detected. In contrast, “intense” luminescence was observed following the reaction of spin-orbit excited $\text{Kr}^+(^2P_{1/2})$ with H_2O ; excited state $\text{H}_2\text{O}^+(\tilde{A}^2A_1)$ products were formed, with the luminescence arising from the $\tilde{A}^2A_1 - \tilde{X}^2B_1$ transition in H_2O^+ . These observations were rationalized by the significant spin-orbit splitting between the $^2P_{3/2}$ and $^2P_{1/2}$ states of Kr^+ and the different Franck-Condon overlap between the reactant and product wave functions. For example, the strongest Franck-Condon factors were identified for the (near-resonant) $\text{Kr}^+(^2P_{1/2}) + \text{H}_2\text{O}$ reactants yielding vibrationally excited $\text{H}_2\text{O}^+(\tilde{A}^2A_1) + \text{Kr}$ products.¹⁵ Spin-orbit selectivity—where, depending on the spin-orbit state of the rare gas ion, H_2O^+ product ions were formed exclusively in the ground or excited electronic state following charge transfer—was also observed in an earlier study involving Ar^+ ions.²³ At the lowest collision energies examined (0.1–0.2 eV), charge transfer cross section measurements for the reaction of Kr^+ with H_2O were found to be in good agreement with both the ADO and parametrized Su capture theory models.

Earlier photoionization spectroscopic studies identified that an electron is removed from the p -type non-bonding b_1 valence orbital centered on the O atom when ground state $\text{H}_2\text{O}^+(\tilde{X}^2B_1)$ ions are formed.²⁴ The p -type orbital is oriented out of the molecular plane, and not along the C_2 axis. Here, *ab initio* calculations identify the most favorable angle of approach for Kr^+ ions to extract an electron from water as occurring when $\theta = \phi = 0^\circ$ (i.e., along the C_2 axis)—where the cation approaches along the dipole axis of the water molecule. To confirm the validity of the reaction mechanism identified from the *ab initio* calculations, additional experimental measurements could be conducted. For example, controlling the

orientation of the H₂O reactants through the application of an external electric field (as recently reported for ammonia molecules)^{25,26} would enable the stereodynamics of the reaction to be established.

Comparison with Other Ion–Molecule Reaction Systems

There have been a number of previous studies into ion–molecule reaction systems under comparable experimental conditions. The astrochemically interesting reaction between sympathetically cooled CCl⁺ ions and thermal CH₃CN neutrals was recently studied within Ca⁺ Coulomb crystals, at an effective reaction temperature of 160 K. The experimental rate coefficient was found to be in agreement with predictions from ADO capture theory.²⁷ For the reaction of non-polar C₂H₂ with CCl⁺ ions, the experimental results were successfully described by the Langevin capture model.²⁸ The relative reactivity of *ortho*- and *para*-water with sympathetically cooled N₂H⁺ ions has also been studied using Coulomb crystals. *Para*-water was found to react faster than *ortho*-water, owing to differences in the dipole moment—as explained within the framework of state-selected, rotationally adiabatic quantum capture theory.²⁹ Capture theories have also successfully described the behavior of ion–molecule reactions studied using methods such as CRESU (cinétique de réaction en écoulement supersonique uniforme, or reaction kinetics in uniform supersonic flow). For example, CRESU measurements performed over a range of low temperatures found the N⁺ + H₂O and N⁺ + NH₃ reaction systems to be well-described by capture theory models.⁴

The experimental rate coefficients measured in this work for the electron transfer between H₂O or D₂O and Kr⁺ are in excellent agreement with ADO capture theory predictions. As highlighted in the preceding paragraph, capture theories have successfully predicted rate coefficients for a range of ion–molecule reaction systems studied under conditions comparable to those adopted in this work. However, this has not always been the case. Recent experimental work on the reactions of ammonia (NH₃ and ND₃) with rare-gas ions (including Kr⁺) found charge transfer to be far slower than capture theory models predicted.^{7,8} An inverse KIE was also observed in the charge transfer between ammonia and rare-gas ions—whereas no KIE is seen in the charge transfer reactions studied in this work.

ADO capture theory rate coefficients can be calculated (in SI units) using the following equation⁷

$$k_{\text{ADO}} = Q \sqrt{\frac{\pi\alpha}{\epsilon_0\mu}} + \frac{Qc\mu_{\text{D}}}{\epsilon_0} \sqrt{\frac{1}{2\pi\mu k_{\text{B}}T}} \quad (1)$$

where Q is the charge on the ion, α is the polarizability of the neutral reactant, ϵ_0 is the permittivity of free space, μ is the reduced mass of the ion–neutral reaction system, μ_{D} is the dipole moment of the neutral species, k_{B} is the Boltzmann constant, and T is the temperature. The c term relates to the average orientation of the dipole of the neutral reactant, according to the ratio $\mu_{\text{D}}/\alpha^{1/2}$, and also depends on the temperature of the system.²⁰ Equation 1 therefore considers several key properties of the polar neutral reactant when predicting the likelihood of the reaction occurring. When comparing the reactions of water and ammonia neutrals with the Kr⁺ ions, these properties are very similar—with the systems featuring comparable dipole moments, polarizabilities, and reduced masses (see Table 2). As such, from a classical capture theory perspective, ammonia and water are expected to

react with Kr⁺ at an approximately equivalent rate. It is therefore very interesting that the reactions of Kr⁺ ions with water isotopologues are in excellent agreement with ADO capture theory predictions, whereas the reactions of Kr⁺ ions with ammonia isotopologues simply cannot be accounted for by any capture theory-based models.

A number of other ion–molecule reaction systems (examined under comparable conditions) have reported rate coefficients that are inconsistent with capture theory calculations. For example, a study between ground-state Be⁺ ions and thermal H₂O, at an effective reaction temperature of 100 K, reported an experimental rate coefficient that was lower than predicted by ADO calculations. A detailed theoretical investigation identified a submerged barrier along the reaction pathway.³⁴ The presence of a submerged barrier along the reaction coordinate is known to affect the likelihood of product formation, as previously demonstrated for reactions between laser-cooled Ca⁺ ions and velocity-selected CH₃F and CH₃Cl neutrals.³⁵ Charge transfer reactions between sympathetically cooled O₂⁺ or N₂⁺ and ground- or excited-state Rb atoms, examined in a hybrid ion-neutral trap, reported an interplay between short- and long-range interactions that depends on the quantum state of the reactants. On the basis of *ab initio* calculations, the strength of the non-adiabatic coupling was shown to govern these effects and, subsequently, the agreement between the experimental findings and classical capture theory predictions. The study concluded that, without the aid of high-level calculations, it is not straightforward to predict the behavior of the different charge transfer systems.³⁶

What this body of work on ion–molecule reaction systems tells us is that—in the absence of experimental measurements or detailed *ab initio* calculations—it is very difficult to predict whether or not capture theory models can accurately account for the behavior of a given ion–molecule reaction system. Theoretical work on the Kr⁺ + H₂O reaction system has identified an avoided crossing between the reactant and product potential surfaces, giving rise to efficient (capture-limited) charge transfer. No energetically accessible crossing point was able to be identified between the reactant and product surfaces in the Kr⁺ + NH₃ reaction system, accounting for the different behavior observed and slower (non-capture-limited) charge transfer.

CONCLUSIONS

Reaction rate coefficients have been measured for the charge transfer reactions between two water isotopologues (H₂O and D₂O) and sympathetically cooled Kr⁺ ions. ADO predictions (a classical capture theory model) are in excellent agreement with the experimental findings, indicating that the reactions are governed by a capture mechanism. High-level *ab initio* calculations have identified a crossing between the reactant and product potential energy surfaces, as anticipated from the experimental findings.

Interestingly, charge transfer reactions between ammonia isotopologues and Kr⁺ ions, undertaken under comparable experimental conditions, behave differently to the water reaction systems. The measured ammonia rate coefficients are suppressed in comparison to capture theory predictions, in contrast to the water reactions examined in this work. Additionally, an inverse KIE effect is observed for the ammonia reactions, with ND₃ reacting faster than NH₃; the two water isotopologues, instead, show very similar reactivities. High-level *ab initio* calculations confirm that the mechanism driving

charge transfer is different when comparing the water and ammonia reaction systems, as no energetically accessible curve crossing was identified for the ammonia reactants. Water and ammonia possess a comparable dipole moment and polarizability, hence they are expected to behave in a similar way (when examined within the framework of capture theory).

Given the lack of experimental data relevant to ISM chemistry, capture theories are often employed in astrochemical models to provide an estimate of rate coefficients of unmeasured ion–molecule reactions. As discussed above, capture theory models do not consistently predict the behavior of a number of ion–molecule reaction systems studied within the framework of Coulomb crystals, even for seemingly “simple” charge transfer reactions. Deviations from capture theory predictions have also been reported when using other experimental techniques, such as CRESU. Hence, the validity of capture theory warrants consideration in each individual reaction system, either via experimental or theoretical means. The need for further work on astrochemically relevant ion–molecule systems is apparent.

■ ASSOCIATED CONTENT

SI Supporting Information

The Supporting Information is available free of charge at <https://pubs.acs.org/doi/10.1021/acsphyschemau.1c00042>.

Calculating the partial pressure of water reactants; calculating rate coefficients; secondary reaction pathways; capture theory calculations (PDF)

■ AUTHOR INFORMATION

Corresponding Author

Brianna R. Heazlewood – Department of Physics, University of Liverpool, Liverpool L69 7ZE, United Kingdom;

orcid.org/0000-0003-2073-4004;

Email: b.r.heazlewood@liverpool.ac.uk

Authors

Andriana Tsikritea – Department of Chemistry, University of Oxford, Physical and Theoretical Chemistry, Oxford OX1 3QZ, United Kingdom; Department of Physics, University of Liverpool, Liverpool L69 7ZE, United Kingdom

Jake A. Diprose – Department of Physics, University of Liverpool, Liverpool L69 7ZE, United Kingdom

Jérôme Loreau – KU Leuven, Department of Chemistry, Leuven B-3001, Belgium; orcid.org/0000-0002-6142-1509

Complete contact information is available at:

<https://pubs.acs.org/doi/10.1021/acsphyschemau.1c00042>

Author Contributions

A.T. and J.A.D. performed the experiments, analyzed the experimental data, and calculated the ADO rate coefficients. B.R.H. devised the project, supervised the experiments, oversaw the data analysis and capture theory calculations, and interpreted the results. J.L. performed the *ab initio* calculations and constructed the potential energy surfaces. All authors contributed to writing the paper.

Notes

The authors declare no competing financial interest.

Data Availability: Supporting data can be obtained from DataCat, the University of Liverpool Research Data Catalogue.

■ ACKNOWLEDGMENTS

B.R.H. acknowledges funding provided by the EPSRC (project EP/N032950/2), the ERC (Starting Grant Project 948373) and the support of the Community for Analytical Measurement Science (CAMS). A.T. thanks the Clarendon Fund for providing her with a scholarship and acknowledges that this paper was supported by the Onassis Foundation, Scholarship ID: F ZP 055-1/2019-2020. J.L. acknowledges support from Internal Funds KU Leuven through Grant STG-19-00313.

■ REFERENCES

- (1) McGuire, B. A. 2018 census of interstellar, circumstellar, extragalactic, protoplanetary disk, and exoplanetary molecules. *Astrophysical Journal Supplement Series* **2018**, *239*, 17.
- (2) Albertsson, T.; Semenov, D. A.; Vasyunin, A. I.; Henning, T.; Herbst, E. New extended deuterium fractionation model: Assessment at dense ISM conditions and sensitivity fractionation analysis. *Astrophysical Journal Supplement Series* **2013**, *207*, 27.
- (3) Clary, D. C. Fast chemical reactions: Theory challenges experiment. *Annu. Rev. Phys. Chem.* **1990**, *41*, 61.
- (4) Marquette, J. B.; Rowe, B. R.; Dupeyrat, G.; Poissant, G.; Rebrion, C. Ion–polar-molecule reactions: A CRESU study of He⁺, C⁺, N⁺ + H₂O, NH₃ at 27, 68 and 163 K. *Chem. Phys. Lett.* **1985**, *122*, 431.
- (5) Wakelam, V.; Smith, I. W. M.; Herbst, E.; Troe, J.; Geppert, W.; Linnartz, H.; Öberg, K.; Roueff, E.; Agúndez, M.; Pernot, P.; et al. Reaction networks for interstellar chemical modelling: improvements and challenges. *Space Science Reviews* **2010**, *156*, 13.
- (6) Heazlewood, B. R.; Softley, T. P. Towards chemistry at absolute zero. *Nature Reviews Chemistry* **2021**, *5*, 125.
- (7) Petralia, L. S.; Tsikritea, A.; Loreau, J.; Softley, T. P.; Heazlewood, B. R. Strong inverse kinetic isotope effect observed in ammonia charge exchange reactions. *Nat. Commun.* **2020**, *11*, 173.
- (8) Tsikritea, A.; Park, K.; Bertier, P.; Loreau, J.; Softley, T. P.; Heazlewood, B. R. Inverse kinetic isotope effects in the charge transfer reactions of ammonia with rare gas ions. *Chemical Science* **2021**, *12*, 10005.
- (9) Lis, D. C.; Roueff, E.; Gerin, M.; Phillips, T. G.; Coudert, L. H.; Van Der Tak, F. F. S.; Schilke, P. Detection of triply deuterated ammonia in the Barnard 1 cloud. *Astrophysical Journal Letters* **2002**, *571*, L55.
- (10) Butner, H. M.; Charnley, S. B.; Ceccarelli, C.; Rodgers, S. D.; Pardo, J. R.; Parise, B.; Cernicharo, J.; Davis, G. R. Discovery of interstellar heavy water. *Astrophysical Journal Letters* **2007**, *659*, L137.
- (11) Heazlewood, B. R. Cold ion chemistry within Coulomb crystals. *Mol. Phys.* **2019**, *117*, 1934.
- (12) Meyer, K. A. E.; Pollum, L. L.; Petralia, L. S.; Tauschinsky, A.; Rennick, C. J.; Softley, T. P.; Heazlewood, B. R. Ejection of Coulomb Crystals from a Linear Paul Ion Trap for Ion–Molecule Reaction Studies. *J. Phys. Chem. A* **2015**, *119*, 12449.
- (13) Jiao, C. Q.; Ranatunga, D. R. A.; Vaughn, W. E.; Freiser, B. S. A pulsed-leak valve for use with ion trapping mass spectrometers. *J. Am. Soc. Mass Spectrom.* **1996**, *7*, 118.
- (14) Jullien, S.; Lemaire, J.; Fenistein, S.; Heninger, M.; Mauclaire, G.; Marx, R. Radiative lifetimes of Xe⁺ and Kr⁺ in their ²P_{1/2} spin-orbit states. *Chem. Phys. Lett.* **1993**, *212*, 340.
- (15) Arnold, S. T.; Dressler, R. A.; Bastian, M. J.; Gardner, J. A.; Murad, E. Dynamics of hyperthermal Kr⁺ + H₂O charge–transfer collisions. *J. Chem. Phys.* **1995**, *102*, 6110.
- (16) Werner, H. J.; Knowles, P. J.; Manby, F. R.; Black, J. A.; Doll, K.; Heßelmann, A.; Kats, D.; Köhn, A.; Korona, T.; Kreplin, D. A.; et al. The Molpro quantum chemistry package. *J. Chem. Phys.* **2020**, *152*, 144107.
- (17) Werner, H. J.; Knowles, P. J. A second order multiconfiguration SCF procedure with optimum convergence. *J. Chem. Phys.* **1985**, *82*, 5053.

- (18) Knowles, P. J.; Werner, H. J. An efficient internally contracted multiconfiguration–reference configuration interaction method. *J. Chem. Phys.* **1988**, *89*, 5803.
- (19) Su, T.; Bowers, M. T. Theory of ion–polar molecule collisions. Comparison with experimental charge transfer reactions of rare gas ions to geometric isomers of difluorobenzene and dichloroethylene. *J. Chem. Phys.* **1973**, *58*, 3027.
- (20) Su, T.; Bowers, M. T. Parameterization of the average dipole orientation theory: temperature dependence. *International Journal of Mass Spectrometry and Ion Processes* **1975**, *17*, 211.
- (21) Okada, K.; Wada, M.; Boesten, L.; Nakamura, T.; Katayama, I.; Ohtani, S. Acceleration of the chemical reaction of trapped Ca^+ ions with H_2O molecules by laser excitation. *Journal of Physics B: Atomic, Molecular and Optical Physics* **2003**, *36*, 33.
- (22) Howard, C. J.; Rundle, H. W.; Kaufman, F. Gas-phase reaction rates of some positive ions with water at 296°K . *J. Chem. Phys.* **1970**, *53*, 3745.
- (23) Dressler, R. A.; Gardner, J. A.; Salter, R. H.; Murad, E. Luminescence measurements of $\text{Ar}^+ + \text{H}_2\text{O}$ and $\text{N}_2^+ + \text{H}_2\text{O}$ suprathermal charge transfer collisions: Product state distributions from $\text{H}_2\text{O}^+ \tilde{A}^2A_1 - \tilde{X}^2B_1$ analysis. *J. Chem. Phys.* **1992**, *96*, 1062–1076.
- (24) Lauzin, C.; Jacovella, U.; Merkt, F. Threshold ionization spectroscopy of H_2O , HDO and D_2O and low-lying vibrational levels of HDO^+ and D_2O^+ . *Mol. Phys.* **2015**, *113*, 3918–3924.
- (25) Steer, E. W.; Petralia, L. S.; Western, C. M.; Heazlewood, B. R.; Softley, T. P. Measurement of the orientation of buffer-gas-cooled, electrostatically-guided ammonia molecules. *J. Mol. Spectrosc.* **2017**, *332*, 94–102.
- (26) Bertier, P.; Heazlewood, B. R. Fringe fields are important when examining molecular orientation in a cold ammonia beam. *Journal of Physics B: Atomic, Molecular and Optical Physics* **2021**, *54*, 205101.
- (27) Krohn, O. A.; Catani, K. J.; Greenberg, J.; Sundar, S. P.; da Silva, G.; Lewandowski, H. J. Isotope-specific reactions of acetonitrile (CH_3CN) with trapped, translationally cold CCl^+ . *J. Chem. Phys.* **2021**, *154*, 074305.
- (28) Catani, K. J.; Greenberg, J.; Saarel, B. V.; Lewandowski, H. J. Reactions of translationally cold trapped CCl^+ with acetylene (C_2H_2). *J. Chem. Phys.* **2020**, *152*, 234310.
- (29) Kilaj, A.; Gao, H.; Rösch, D.; Rivero, U.; Küpper, J.; Willitsch, S. Observation of different reactivities of *para* and *ortho*-water towards trapped diazenylium ions. *Nat. Commun.* **2018**, *9*, 2096.
- (30) Wolfsberg, M.; Van Hook, W. A.; Paneth, P.; Rebelo, L. P. N. In *Isotope effects: in the chemical, geological, and bio sciences*; Springer Science & Business Media, 2009; p 392.
- (31) Woodin, R. L.; Beauchamp, J. L. Binding of Li^+ ion to Lewis bases in the gas phase. Reversals in methyl substituent effects for different reference acids. *J. Am. Chem. Soc.* **1978**, *100*, 501.
- (32) Halevi, E. A.; Haran, E. N.; Ravid, B. Dipole moment and polarizability differences between NH_3 and ND_3 . *Chem. Phys. Lett.* **1967**, *1*, 475.
- (33) Hollas, J. M. In *Modern spectroscopy*; John Wiley & Sons, 2004; p 98.
- (34) Yang, T.; Li, A.; Chen, G. K.; Xie, C.; Suits, A. G.; Campbell, W. C.; Guo, H.; Hudson, E. R. Optical control of reactions between water and laser-cooled Be^+ ions. *J. Phys. Chem. Lett.* **2018**, *9*, 3555.
- (35) Gingell, A. D.; Bell, M. T.; Oldham, J. M.; Softley, T. P.; Harvey, J. N. Cold chemistry with electronically excited Ca^+ Coulomb crystals. *J. Chem. Phys.* **2010**, *133*, 194302.
- (36) Dörfler, A. D.; Eberle, P.; Koner, D.; Tomza, M.; Meuwly, M.; Willitsch, S. Long-range versus short-range effects in cold molecular ion-neutral collisions. *Nat. Commun.* **2019**, *10*, 5429.